



Housing and Building National Research Center

HBRC Journal

<http://ees.elsevier.com/hbrcj>

Experimental study on the determination of small strain-shear modulus of loess soil



Mona El Mosallamy ^{a,*}, Tarek T. Abd El Fattah ^a, Mohammed El Khouly ^b

^a National Research Centre, Egypt

^b Cairo University, Egypt

Received 1 January 2014; revised 26 October 2014; accepted 24 November 2014

KEYWORDS

Oedometer;
Resonant column;
Loess;
Maximum shear modulus;
Damping ratio

Abstract The primary aim of this study was to investigate the collapse potential of loess soil in Egypt, the factors affecting the dynamic properties of this soil and establish relationships between them. Whether engineered or natural, may exist in seismic zones; or may be subjected to small strain vibrations, therefore, there is a need to assess the wetting dynamic properties of collapsible soils.

A series of oedometer and resonant column tests were conducted to study the effect of applied pressure, void ratio, water content and silt content on the collapse potential (C_p), maximum shear modulus (G_{max}) and damping ratio (D_T) of the tested samples. The results indicate significant increase in the collapse potential and reduction in (G_{max}) with the increase of silt content. The results, also, indicate that the (C_p) is less for sample with higher initial relative densities and initial water content.

Test results also show that (G_{max}) increases with the increase of confining pressure and relative density. The change in damping properties is not significant under the effect of silt content and water content, and it reduces slightly with the increase of confining pressure and relative density. Empirical equations based on the results of the experimental work were proposed to predict (G_{max}) with respect to (C_p), voids ratio and applied pressure.

© 2014 Production and hosting by Elsevier B.V. on behalf of Housing and Building National Research Center. This is an open access article under the CC BY-NC-ND license (<http://creativecommons.org/licenses/by-nc-nd/4.0/>).

Introduction

Loess soils can be defined as the soil which can exhibit a large settlement with or without increase in the applied stress upon wetting. This volume change is usually associated with change in soil structure. Loess soil covers approximately 10% of the Earth's land mass [1].

In Egypt, recent extensions of urban communities towards the desert have exposed Egyptian geotechnical engineers to relatively new challenges, among which is dealing with loess soil.

Abbreviations: G_{max} , maximum shear modulus; D_T , damping ratio; C_p , collapse potential; τ_d , shear stress; σ_{vo} , normal stress; G_s , specific gravity; R_D , relative density; w_c , water content.

* Corresponding author.

Peer review under responsibility of Housing and Building National Research Center.



Production and hosting by Elsevier

<http://dx.doi.org/10.1016/j.hbrcj.2014.11.010>

1687-4048 © 2014 Production and hosting by Elsevier B.V. on behalf of Housing and Building National Research Center.

This is an open access article under the CC BY-NC-ND license (<http://creativecommons.org/licenses/by-nc-nd/4.0/>).

Loess soils are observed in many areas in Egypt. Most of these areas are situated in the western desert which covers about 65% of the area of Egypt. From the previous studies, it can be concluded that most of the loess soils in Egypt were deposited in shallow water depths in a loose structure of high void ratio. Rivers, flood streams and rainfalls are responsible for these formations.

Detecting the dynamic settlement potential of this soil is misleading during site investigation due to cementation and negative pore pressures which causes high strength. The extent of the problem could be significant in regions where loess soils are widespread and the seismic activity is great and especially where the collapse has been triggered by rising ground water table.

Gibbs and Bara [2] studied a collapsible potential of loess soil which subjected to cyclic loading and their results show that 10% reduction in shear strength parameters (c and ϕ) is observed due to cyclic loading equivalent to a 0.39 g. Parkash and Puri [3] tested undisturbed samples of loess from Memphis (USA) under cyclic triaxial conditions. They observed that in these types of soils the development of large axial strain and pore pressure build-up go together. They also found that the number of cycles of loading required to induce liquefaction was large for the loessial silt soils compared to clean sands. This was explained by the presence of cohesion in the loessial soils which delayed the build-up of pore water pressures.

Bahatia and Quasts [4] performed a series of static and cyclic triaxial tests on fabricated and undisturbed samples under natural moisture content and saturated conditions to study the effect of soil structure on the static and cyclic behaviour of soils. The most recent material to be deposited in this area is the alluvium; these deposits then dried out and never again become saturated. They observed that the structure of collapsible soil helped to increase the resistance to deformations under both static and cyclic loading as long as the soil was tested under the natural moisture content. If the soil was saturated, the collapsible soil structure was broken down and the soil did not show any increased resistance to deformation but behave like any loose soil. It is also noticed that the fabricated samples experienced larger strains than undisturbed samples for the same deviatoric stress.

Ishihara and Harada [5] conducted a series of cyclic simple shear tests on local Japanese soils to examine the influence of collapse on liquefaction or cyclic softening characteristics of reconstituted partially saturated samples with different histories of collapse. They found that the cyclic stress ratio (τ_{dl}/σ'_{vo}) needed to induce a state of cyclic softening under a given number of cycles depends on the collapse potential experienced by the samples prior to the application of cyclic load especially at relatively low number of cycles (< 10). In other words, the greater the collapse potential, the smaller the cyclic stress ratio required to causing cyclic softening.

Laboratory testing programme

Materials

Samples used in this research were obtained from the site of the underground metro – fourth stage – 6 October City at the link between the Ring road and Wahat road. Figs. 1 and

2 show the location of the study area by Google Earth and a cross sections in the natural soil of the study area.

Some of the natural samples obtained for this research were washed on No. 200 sieve in order to separate the fines from the sand to be able to use different portions out of fines in the study. Four mixtures of samples were prepared with fines contents of 0%, 10%, 20%, and 30%. Other samples were left for undisturbed testing.

The physical properties of the tested soil were determined according to ASTM standards. Test results are summarized in Table 1 and Figs. 3 and 4.

Testing techniques

Oedometer tests

In order to study the collapse potential and the stress strain behaviour of tested soils, laboratory tests were carried out by means of conventional oedometer device using remoulded samples. Samples were of 6.0 cm diameter and 2.4 cm height. The tested soil mixture was placed in the oedometer ring in 4 layers each of 5 to 6 mm and compacted using wooden dolly, in order to achieve the desired relative density. The moisture content varies according to the testing programme. Several attempts were carried out for the target relative density to be reached.

Resonant column test

The resonant column test is used for measuring the low-strain dynamic properties of soils by vibrating a cylindrical soil specimen in a fundamental mode of vibration, in torsion or flexure [6]. Once the fundamental mode is established, the resonant frequency and amplitude of vibration are measured. This fixed-free configuration system is capable of testing a cylindrical specimen in torsion at its fundamental frequency by a drive system. From measuring the motion of the free end, and the velocity of the propagating wave, the degree of material damping can be derived. The shear modulus is then obtained from the derived velocity and the density of the sample. Figs. 5

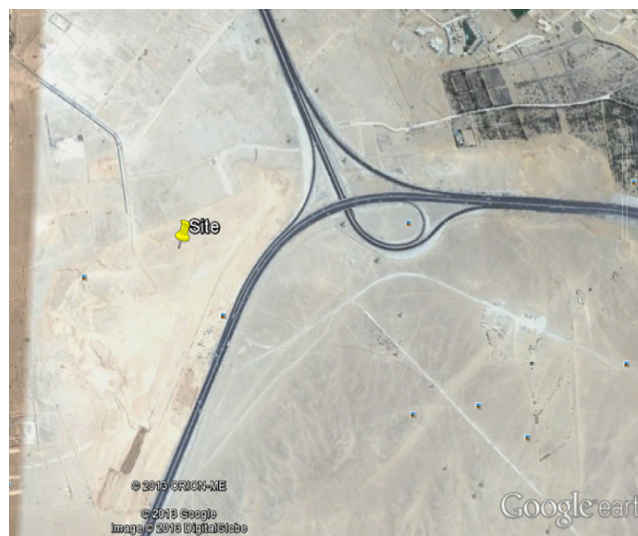


Figure 1 Study area by Google earth.



Figure 2 Cross-sections in the study area.

Table 1 Summary of physical properties of tested samples.

Samples	1	2	3	4
Maximum dry density (kN/m ³)	19.8	20.3	19.8	19.3
Minimum dry density (kN/m ³)	15.3	14.8	14.3	13.1
Minimum void ratio (e_{min})	0.33	0.3	0.32	0.38
Maximum void ratio (e_{max})	0.72	0.77	0.85	1.04
G_s	2.63	2.63	2.65	2.66
Gravel (%)	4.5	4.5	4	4
Sand (%)	95.5	85.5	76	66
Silt (%)	0	10	20	30
D_{10} (mm)	0.14	0.075	0.045	0.04
D_{30} (mm)	0.23	0.2	0.16	0.07
D_{60} (mm)	0.44	0.4	0.35	0.3
Cu	3.14	5.33	7.78	7.5
Cc	0.86	1.33	1.63	0.41
<i>For fine materials</i>				
Liquid limit (%)	NA	18	23	30
Plastic limit (%)	NA	10	13	15

and 6 show a schematic diagram for the device and the used GDS machine (GDS) [7].

The resonant column test is performed according to ASTM standards D4015 by applying a sinusoidal torque via an electromagnetic drive system to the specimen. The drive system consists of a four-arm rotor that has a permanent magnet fitted to the end of each arm and a support cylinder to which four pairs of wire coils are fitted.

This produces an oscillatory motion in the drive plate due to the resultant magnetic field. By controlling the frequency and amplitude of the applied voltage, the resonant frequency of the specimen can be found. The amplitude of the vibration is monitored by the output of an accelerometer that is attached to the drive plate as a sweep of applied frequencies is undertaken.

Testing programme

The testing procedure comprised of two main groups: studying the effect of confining pressure with constant initial water

content and studying the effect of initial water content with constant confining pressure. A summary of each testing group is provided in Tables 2 and 3.

Results and analysis

This section aims at presenting the results and analysing the data obtained from various tests conducted in Resonant Column test and Oedometer test to highlight some of the factors affecting the dynamic properties and the settlement due to inundation of different silty-sand soil mixtures.

Also correlations between the dynamic shear modulus and the collapse potential were conducted.

Oedometer test results

Various tests have been conducted using different silt content mixtures. The objective of these tests is to highlight the effect of silt content, initial relative density, water content and inundation pressure on the collapse potential of soil.

The oedometer tests were divided into two groups. Group “A” is to study the effect of applied stress at inundation using soil samples with different silt contents and different initial relative densities and with same initial water content of 3%, which represents the natural water content of the natural undisturbed samples. Group “B” is to study the effect of the initial water content using soil mixtures of silt content of 20% and different initial relative densities at the same inundation pressure of 200 kPa [8].

Group A

These tests were conducted on samples of silt contents of 0%, 10%, 20% and 30%, relative densities of 20%, 40% and 60%, inundation pressures of 50 kPa, 100 kPa, 200 kPa and 250 kPa and initial water content of 3%.

Figs. 7–10 show the collapse potential versus the inundation pressure for the tested samples. From figures, the collapse potential increases with the increase of silt content, its value increases from 1.2% for sample with silt content 0% and relative density 60% at inundation pressure of 50 kPa, to 7% for sample with silt content 30% and relative density 20% at inundation pressure of 250 kPa. It is, also, clear that the collapse potential increases with the increase of inundation pressure, silt content and decreases with the increase of initial relative density.

Group B

These tests were conducted on samples of silt contents 20%, relative densities of 20%, 40% and 60%, inundation pressure of 200 kPa and initial water contents of 0%, 3%, 6% and 9%.

Fig. 11 shows the significance of the initial water content on the collapse potential. This figure indicates that the wetter the soils were at compaction, the lower the collapse potential. The collapse potential is reduced because the initial bond provided by the fine fractions in the soil has already broken due to the higher initial amount of water. In other words, higher initial water content reduces the bonding forces, and what remains from these forces to be reduced completely by wetting is less; as a result, less collapse would occur.

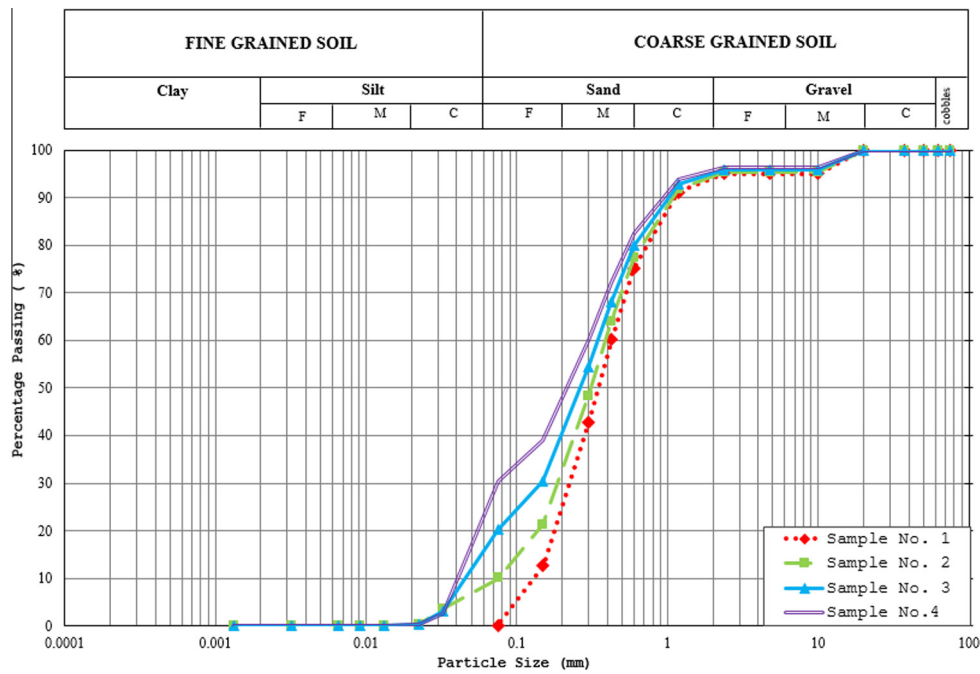


Figure 3 Grain size distributions of tested samples with different silt contents.

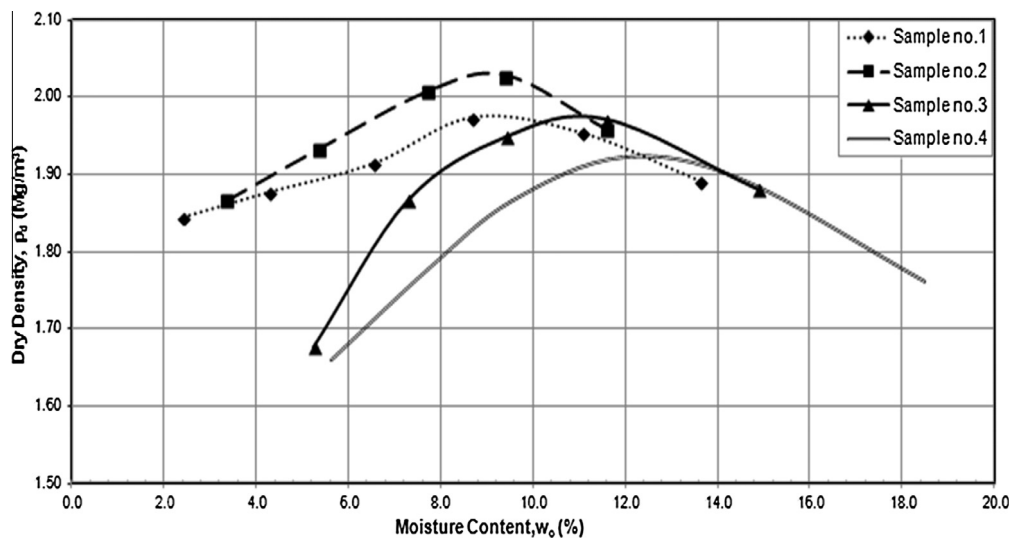


Figure 4 Compaction tests for soil samples.

Resonant column test results

Various tests have been conducted on re-moulded samples with different silt content mixtures. The objective of these tests is to highlight the effect of silt content, initial relative density, initial water content and confining pressure on the dynamic shear properties of soil specifically, small strain shear modulus (G_{max}) and damping ratio (D_T).

The resonant column tests were divided into two groups. Group “A” is to study the effect of the confining pressure. The tested samples were with different silt contents, different initial relative densities and the same initial water content of

3%. Group “B” is to study the effect of initial water content. The tested samples were with silt content of 20% and with different initial relative densities and tested at the same confining pressure of 200 kPa [8].

Group A

Torsional and damping tests were conducted on samples of 5.0 cm diameter and 10.0 cm height with silt contents of 0%, 10%, 20% and 30%, relative densities of 20%, 40% and 60%, confining pressures of 50 kPa, 100 kPa, 200 kPa and 250 kPa and initial water content of 3%.

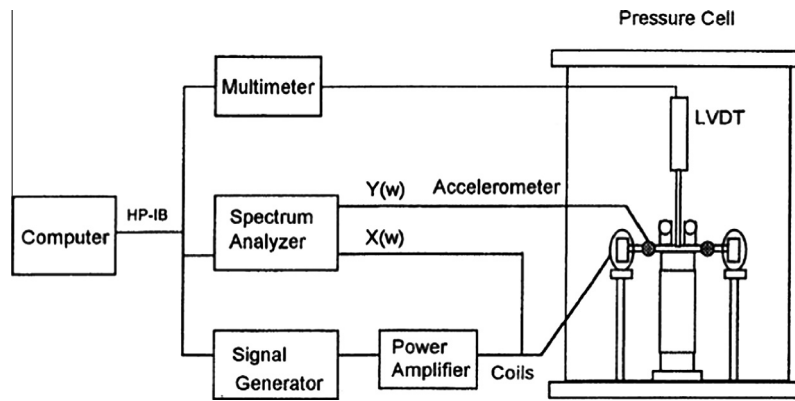


Figure 5 Schematic diagram for Resonant Column device [6].

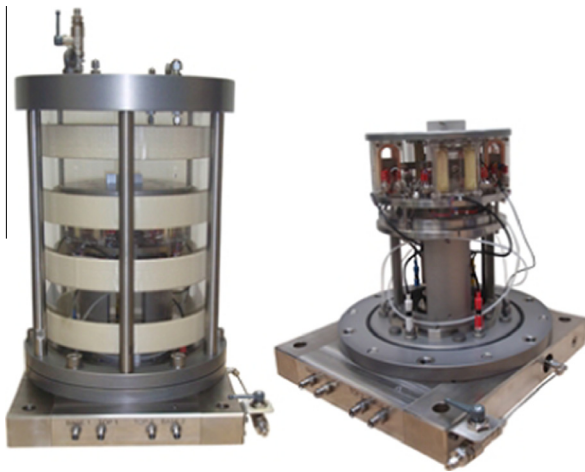


Figure 6 The used GDS Resonant Column device.

Table 3 Experimental programme for group (B).

Silt content (%)	R_D (%)	w_c (%)			
20	20	0	3	6	9
	40	0	3	6	9
	60	0	3	6	9

confinement and relative density. It is also, decreased with higher silt content.

After applying torsional resonance and conducting the resonance frequency for G_{max} , a damping test was carried out to measure the damping ratio corresponding to this resonant frequency.

Figs. 16–19 show the trend of the damping ratio with respect to confining pressure. The figures show that the damping ratios range from 1% to 2.5%. For samples with the same silt content, damping ratio decreases with the increase of confining pressure and increases with increase of relative density.

These figures, also, show that the change in damping ratio in samples with different silt contents is very small that it can be neglected.

Group B

Torsional and damping tests were conducted on samples with silt content of 20%, relative densities of 20%, 40% and 60%, confining pressures of 200 kPa and initial water contents of 0%, 3%, 6% and 9%.

Resonant frequencies at low shear strain ($\approx 0.001\%$) were measured until the value settles at each confinement level; damping ratio was also investigated with torsional resonant frequency.

Figs. 20 and 21 show the calculated G_{max} and measured damping ratio for the tested soil mixture with different relative densities measured by the resonant column at low strain ($\approx 0.001\%$).

It is noticed from these figures that the dynamic shear modulus increases slightly with the increase of water content and the rate of increase is more in case of mixtures with low relative density. The change in the damping ratio is very small that it can be considered that the effect of water content on the damping ratio can be neglected.

In general, the effect of water content on the dynamic properties of soil is very small and it is more effective in case of mixtures with low relative densities.

Table 2 Experimental programme for group (A).

Silt content (%)	R_D (%)	σ (kPa)			
0	20	50	100	200	250
	40	50	100	200	250
	60	50	100	200	250
10	20	50	100	200	250
	40	50	100	200	250
	60	50	100	200	250
20	20	50	100	200	250
	40	50	100	200	250
	60	50	100	200	250
30	20	50	100	200	250
	40	50	100	200	250
	60	50	100	200	250

Resonant frequencies at low shear strain ($\approx 0.001\%$) were measured until the value settles at each confinement level; damping ratio was also investigated with torsional resonant frequency.

Figs. 12–15 show the variation of G_{max} with confining pressure and initial relative density. From these figures, the low strain shear modulus increases with the increase of the

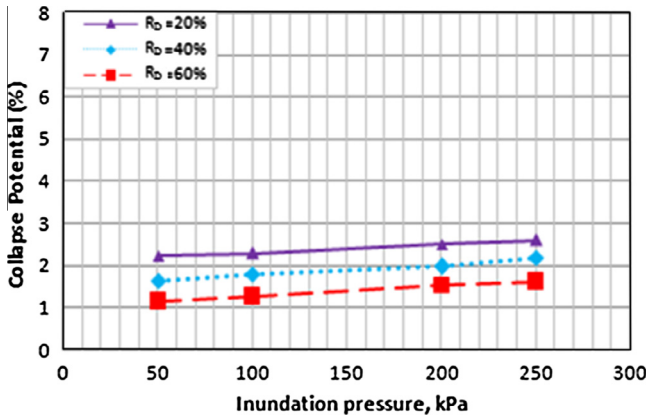


Figure 7 Collapse potential versus inundation pressure for soil mixture of silt content of 0%.

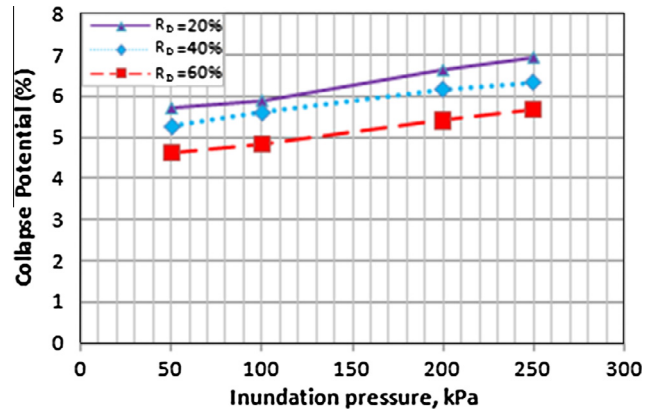


Figure 10 Collapse potential versus inundation pressure for soil mixture of silt content of 30% with different relative densities.

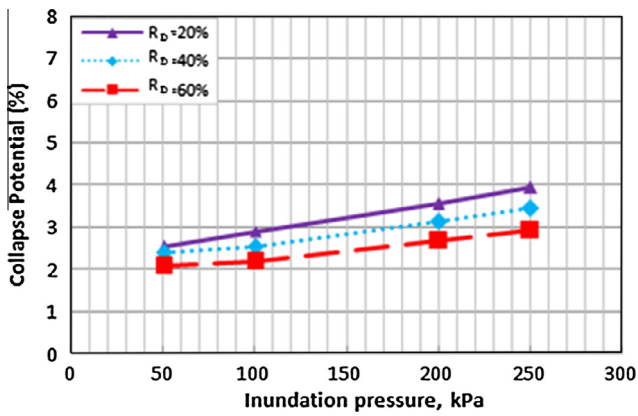


Figure 8 Collapse potential versus inundation pressure for soil mixture of silt content of 10% with different relative densities.

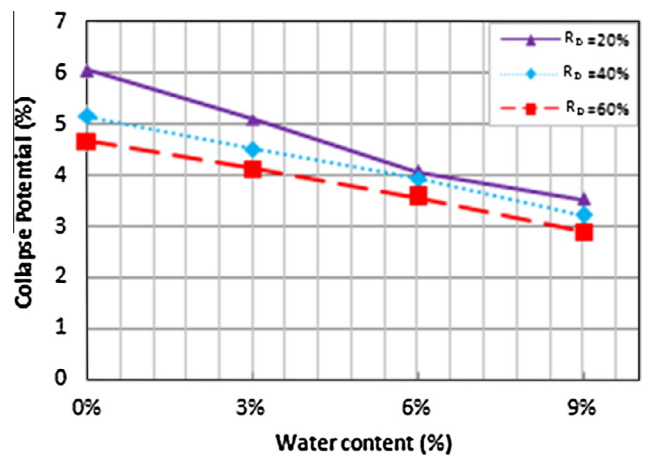


Figure 11 Collapse potential versus water content for soil mixture of silt content of 20%.

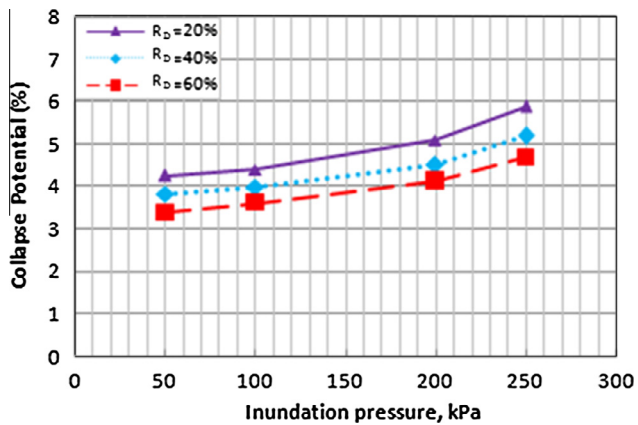


Figure 9 Collapse potential versus inundation pressure for soil mixture of silt content of 20% with different relative densities.

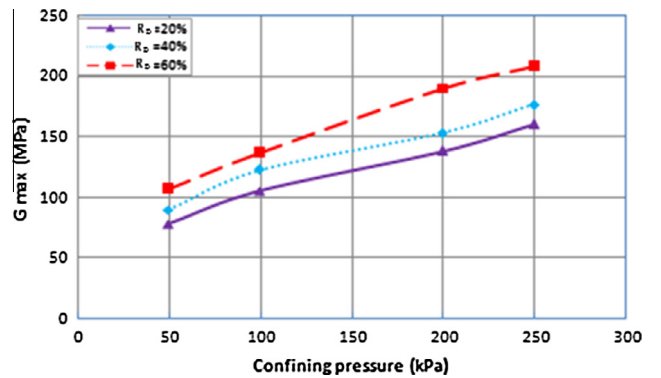


Figure 12 G_{max} versus confining pressure for soil mixture of silt content of 0% with different relative densities.

Correlation between collapse potential and dynamic shear properties

Figs. 22–25 show the relationship between collapse potential of soil mixtures with different silt contents and relative densities

at inundation pressures of 50 kPa, 100 kPa, 200 kPa and 250 kPa, versus the low strain dynamic shear modulus of the same soil mixtures at the same confining pressures.

The points of each soil mixture have almost the same trend as the R^2 values of the best fit line are very close to 1, therefore

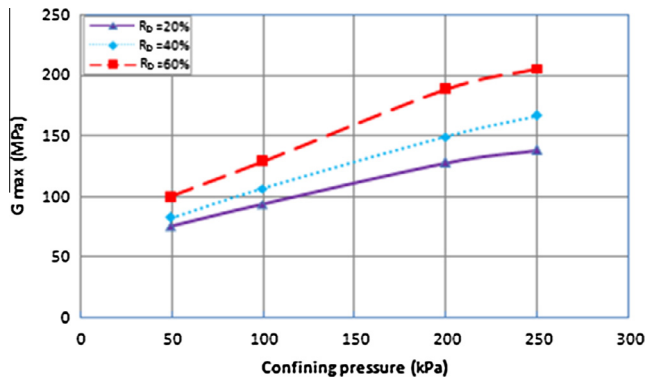


Figure 13 G_{max} versus confining pressure for soil mixture of silt content of 10% with different relative densities.

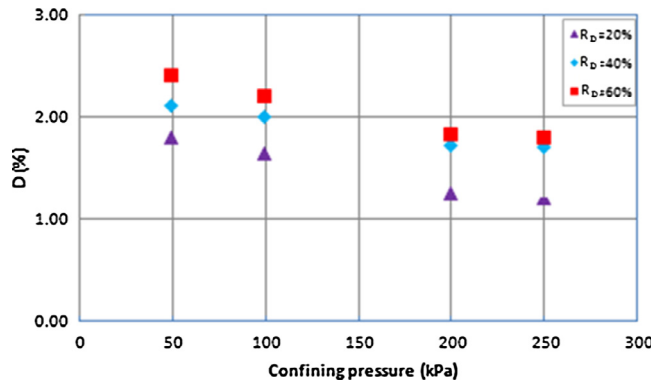


Figure 16 Damping ratio versus confining pressure for soil mixture of silt content of 0% with different relative densities.

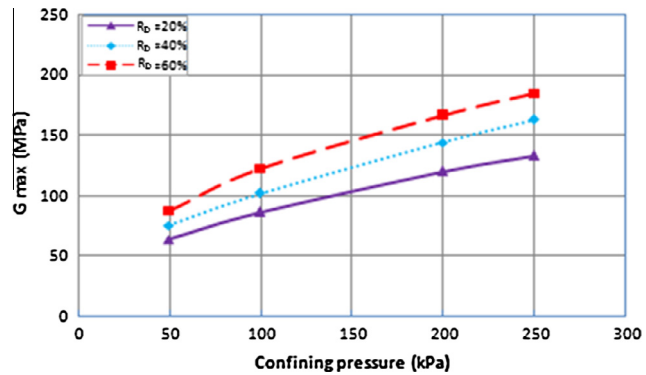


Figure 14 G_{max} versus confining pressure for soil mixture of silt content of 20% with different relative densities.

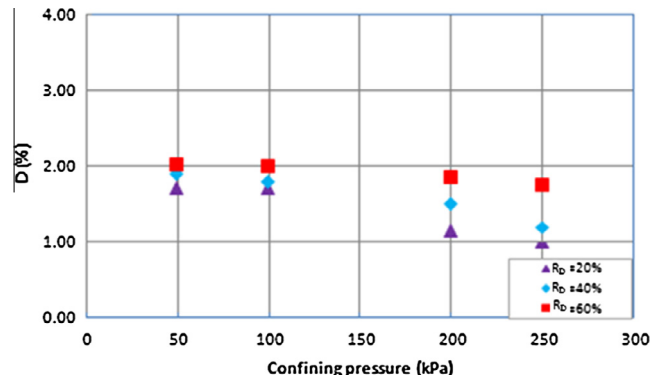


Figure 17 Damping ratio versus confining pressure for soil mixture of silt content of 10% with different relative densities.

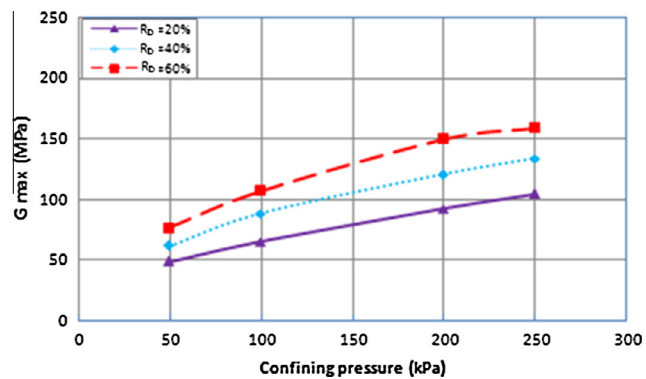


Figure 15 G_{max} versus confining pressure for soil mixture of silt content of 30% with different relative densities.

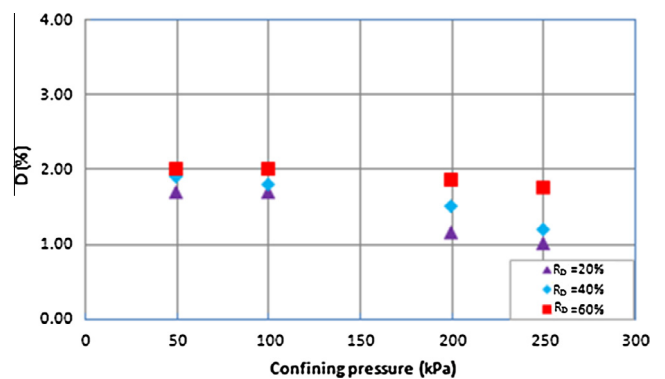


Figure 18 Damping ratio versus confining pressure for soil mixture of silt content of 20% with different relative densities.

the values can be considered as a good explanation for the correlation.

These figures show that G_{max} decreases with the increase of collapse potential (C_p) for a soil mixture of a certain silt content, and G_{max} and C_p are increasing with the increase of applied pressure.

G_{max} also increases with the increase of relative density, and it decreases with the increase of silt content. The collapse potential decreases significantly with denser soil mixtures.

The more the silt contents in tested samples, the more the collapse potential and the less G_{max} have resulted.

Regression analysis for G_{max}

In order to better understand the effect of different parameters on C_p and G_{max} , non-linear regression analysis was done using Statgraphics software to get these relationships.

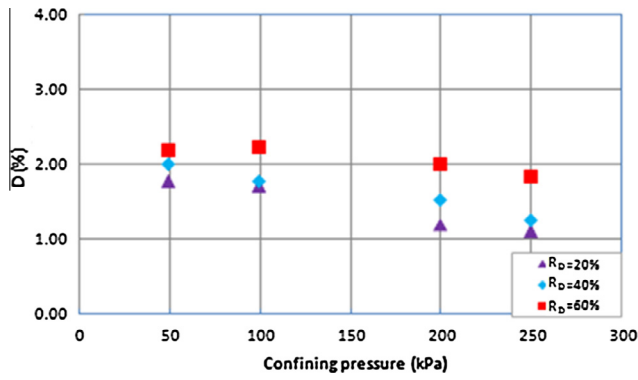


Figure 19 Damping ratio versus confining pressure for soil mixture of silt content of 30% with different relative densities.

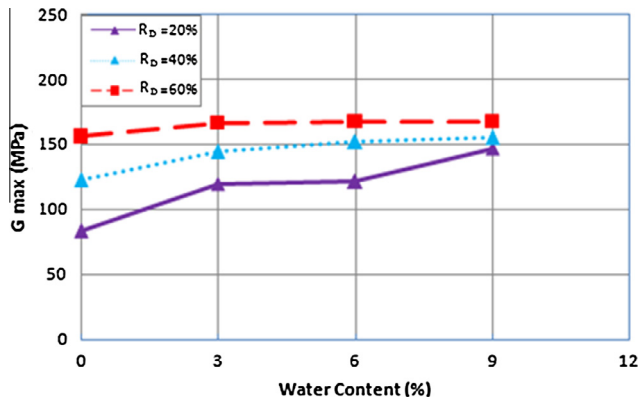


Figure 20 Relationship between G_{max} and water content for soil mixture of silt content of 20% with different relative densities.

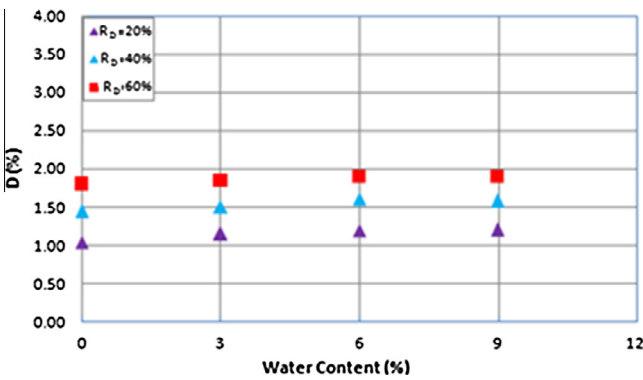


Figure 21 Relationship between D and water content for soil mixture of silt content of 20% with different relative densities.

The dependent parameter is G_{max} , and the independent parameters are C_p , σ , R_D and silt content, these empirical equations are not reliable in considering the effect of silt content, so, individual equations for each silt content was derived. These relationships are as follows:

1. For silt content = 0%

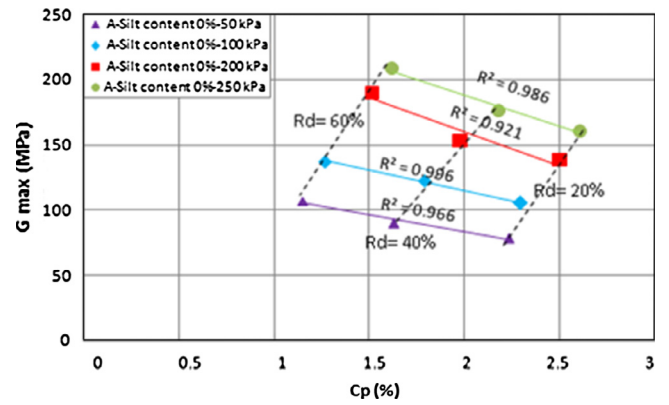


Figure 22 Relationship between collapse potential (C_p) and G_{max} for soil mixtures of 0% silt content.

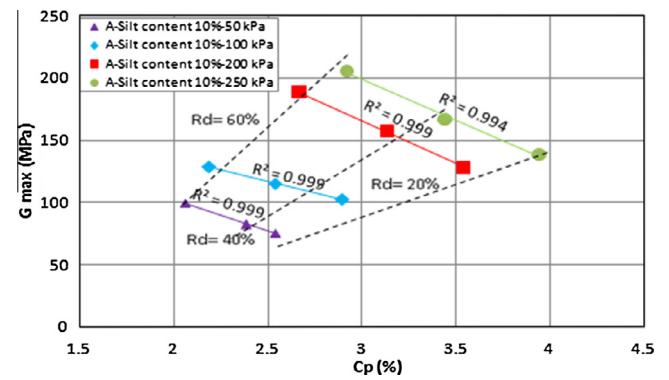


Figure 23 Relationship between collapse potential (C_p) and G_{max} for soil mixtures of 10% silt content.

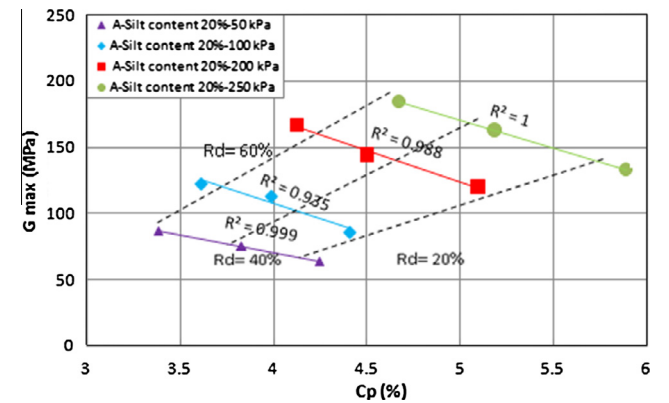


Figure 24 Relationship between collapse potential (C_p) and G_{max} for soil mixtures of 20% silt content.

$$G_{max} = 4.43(C_p + 1.9) \frac{(1.62 - e)^2}{(1 + e)} \sigma^{0.5} \quad (1)$$

where G_{max} dynamic shear modulus (MPa), C_p collapse potential (%), σ inundation pressure (kPa) and e voids ratio.

Fig. 26 shows the shear modulus versus the collapse potential from the test results and the calculated values from the

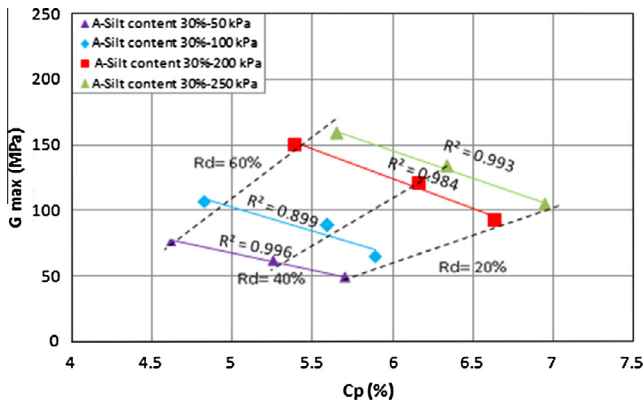


Figure 25 Relationship between collapse potential (C_p) and G_{max} for soil mixtures of 30% silt content.

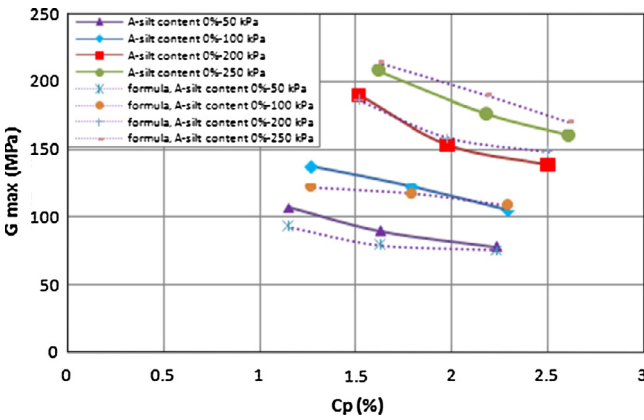


Figure 26 Shear modulus versus collapse potential from the test results and the calculated values from the proposed empirical formula for mixture with 0% silt content.

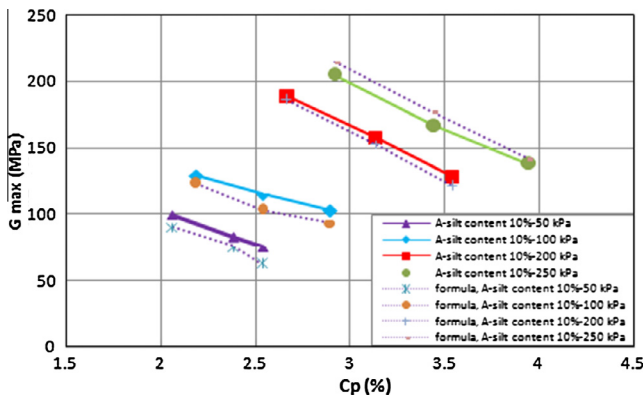


Figure 27 Shear modulus versus collapse potential from the test results and the calculated values from the proposed empirical formula for mixture with 10% silt content.

proposed empirical formula for the soil mixture with 0% silt content and the results are in good agreement.

2. For silt content = 10%

$$G_{max} = 2.431(C_p + 5.032) \frac{(1.51 - e)^2}{(1 + e)} \sigma^{0.5} \quad (2)$$

where G_{max} dynamic shear modulus (MPa), C_p collapse potential (%), σ inundation pressure (kPa) and e voids ratio.

Fig. 27 shows the shear modulus versus the collapse potential from the test results and the calculated values from the proposed empirical formula for the soil mixture with 10% silt content and the results are in good agreement.

3. For silt contents = 20% & 30%

$$G_{max} = 3.896(C_p + 10.644) \frac{(1.72 - e)^2}{(1 + e)} \sigma^{0.5} \quad (3)$$

where G_{max} dynamic shear modulus (MPa), C_p collapse potential (%), σ inundation pressure (kPa) and e Voids ratio.

Figs. 28 and 29 show the shear modulus versus the collapse potential from the test results and the calculated values from

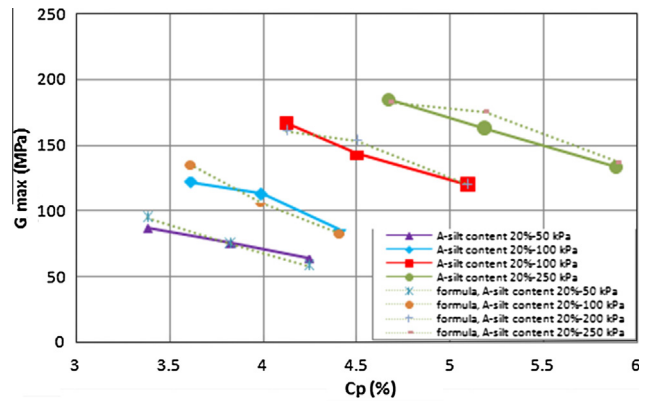


Figure 28 Shear modulus versus collapse potential from the test results and the calculated values from the proposed empirical formula for mixture with 20% silt content.

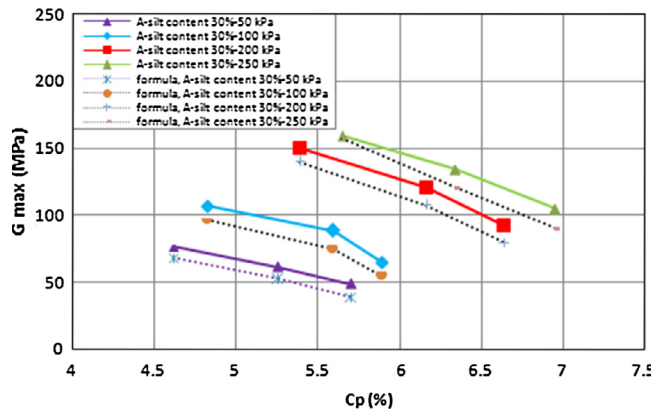


Figure 29 Shear modulus versus collapse potential from the test results and the calculated values from the proposed empirical formula for mixture with 30% silt content.

the proposed empirical formula for the soil mixture with 20% and 30% silt contents and the results are in good agreement.

Conclusions

This research has focused on the collapse behaviour and dynamic properties of loess deposits. These parameters have been reviewed, investigated and discussed. Special attention was paid to the influence of silt content, relative density and applied pressure. Two different experimental programmes have been employed to investigate the collapse behaviour and the low strain dynamic shear properties of loess soil.

The main conclusions derived from this research are as follows:

1. From the results of Oedometer tests, the collapse potential (C_p) of soil increases with the increase of silt content as it moves from the moderate problems in samples that have no silt to trouble in samples with silt content of 30%. (C_p) also increases with the increase of applied pressure and decreases with the increase of initial relative density and initial water content.
2. From the results of Resonant Column tests. The resonant frequency increases with the increase of confining pressure, the rate of increasing is slightly higher at low stresses and lower relative densities.
3. The dynamic shear modulus increases with the increase of confining pressure and with the decrease of silt content.
4. The damping ratio (D) slightly decreases with the increase of confining pressure.
5. The low strain dynamic shear modulus (G_{max}) slightly increases with the increase of water content and the rate of increase is more for samples prepared at lower relative density.
6. The effect of water content on the damping ratio is negligible.
7. The low strain dynamic shear modulus (G_{max}) decreases with the increase of silt content.
8. The silt content has almost no effect on the damping ratio of the tested samples when all other parameters are kept constant.
9. The low strain dynamic shear modulus (G_{max}) increases with the increase of collapse potential for samples of a certain silt content and relative density. This is due to the increase of applied stresses which causes increase in both C_p and G_{max} .
10. The low strain dynamic shear modulus (G_{max}) increases with the increase of relative density which is contrary to what happened in collapse potential which decreases significantly with the increase of relative density.

11. For samples prepared at silt contents of 0%, 10%, 20% and 30% , the more the silt content is, the more the collapse potential and the less G_{max} .
12. Damping ratio decreases with the increase of C_p when the silt content and relative density are kept constant, as a result of increase of applied pressure.
13. Damping ratio increases with the decrease of C_p for soil samples with more relative densities. It also, slightly decreases with the increase of C_p for soil samples with more silt content.

Used ASTM standards

1. D854 Test Methods for Specific Gravity of Soil Solids by Water Pycnometer.
2. D2216 Test Methods for Laboratory Determination of Water (Moisture) Content of Soil and Rock by Mass.
3. D6913 Test Methods for Particle-Size Distribution (Gradation) of Soils Using Sieve Analysis.
4. D1557 Standard Test Methods for Laboratory Compaction Characteristics of Soil Using Modified Effort.
5. D4254 Standard Test Methods for Minimum Index Density and Unit Weight of Soils and Calculation of Relative Density.
6. D4015 Standard Test Methods for Modulus and Damping of Soils by Resonant-Column Method.

References

- [1] I. Jefferson, M. Ahmad, [Formation of artificial collapsible loess, Problematic Soils Rocks In Situ Charact. \(2007\) 1–10](#)
- [2] H.J. Gibbs, J.P. Bara, Predicting surface subsidence from basic soil tests. Special Technical publication (STP), Am. Soc. Test. Mater. (ASTM) 322 (1962) 231–247.
- [3] S. Parkash, V.K. Puri, Liquefaction of loessial soils, in: Third International Earthquake Microzonation Conference Proceedings, vol. 2, Seattle, Washington, 1982, pp. 1101–1107.
- [4] S.K. Bhatia, D. Quast, The behaviour of collapsible soil under cyclic loading, in: Fourth Australia–New Zealand Conference on Geomechanics Perth, 1984, pp. 73–77.
- [5] K. Ishihara, K. Harada, Cyclic behavior of partially saturated collapsible soils subjected to water permeation. Ground failures under seismic conditions, Geotechnical Special publication, ASCE, Atlanta, GA, USA, 1994, pp. 34–50.
- [6] G. Cascante, C. Santamarina, N. Yassir, [Flexural excitation in a standard torsional-resonant column device, Can. Geotech. J. 35 \(1998\) 478–490.](#)
- [7] GDS Resonant Column System Operation Manual.
- [8] M. El Mosallamy, Experimental study on dynamic behaviour of collapsible soil, M.Sc Thesis, Cairo University, 2013.